

## Research Article

# Raman Spectroscopy-Assisted Characterization of Nanoform MoS<sub>2</sub> Thin Film Transistor

Rajasekaran Saminathan <sup>1</sup>, Haitham Hadidi,<sup>1</sup> Mohammed Tharwan <sup>1</sup>, Ali Alnujaie,<sup>1</sup>  
Jabril A. Khamaj,<sup>1</sup> and Gunasekaran Venugopal <sup>2</sup>

<sup>1</sup>Mechanical Engineering Department, Faculty of Engineering, Jazan University, P. O. Box 45142, Jazan, Saudi Arabia

<sup>2</sup>Department of Materials Science, School of Technology, Central University of Tamil Nadu, Thiruvavur, 610005 Tamil Nadu, India

Correspondence should be addressed to Gunasekaran Venugopal; [gunasekaran@cutn.ac.in](mailto:gunasekaran@cutn.ac.in)

Received 16 January 2022; Revised 22 May 2022; Accepted 30 May 2022; Published 22 June 2022

Academic Editor: Zhichao Lou

Copyright © 2022 Rajasekaran Saminathan et al. This is an open access article distributed under the Creative Commons Attribution License, which permits unrestricted use, distribution, and reproduction in any medium, provided the original work is properly cited.

In this paper, we report the simple preparation and investigation of electrical transport properties of nanoform MoS<sub>2</sub> thin film transistor (TFT) devices. MoS<sub>2</sub> nanoparticles were synthesized by using the hydrothermal method. The physiochemical characterizations such as UV-vis, Fourier transform infrared, X-ray diffraction, and Raman spectroscopy studies were performed. Spin-coating was used to make the thin film on which silver electrodes were made. We observed nonlinear current-voltage (I-V) characteristics; however, the symmetricity was found in the I-V curve which confirms the no formation of the Schottky barrier between thin film and electrodes. Transistor transfer characteristics reveal that the TFT device is n-doped as more drain current modulation is observed when the positive gate voltage is applied. The relationship between gate-current and gate voltage studies concludes that there is no leakage gate current in the TFT device which further confirms the good reliability of transfer characteristics of a device. The device mobility was calculated as  $\sim 10.2 \text{ cm}^2/\text{Vs}$ , and the same was explained with plausible reason supported with Raman spectra analysis.

## 1. Introduction

Presently, two-dimensional materials (graphene, graphene-oxide, MoS<sub>2</sub>, and Bi<sub>2</sub>Se<sub>3</sub>) have been known for their unique characteristics and having potential prospects in various fields such as electronics, photovoltaic, sensors, flexible displays, supercapacitors, and water purification [1, 2]. Transition metal dichalcogenide semiconductors (TMDC) have significantly attracted the scientific community because of their unique electrical and optical characteristics. Molybdenum disulfide (MoS<sub>2</sub>) is a layered structure transition metal dichalcogenide material with weak van der Waals interlayer force, which is considered as a best candidate material for numerous applications such as supercapacitor, hydrogen generation/storage, photocatalyst, and rechargeable batteries [3–8]. MoS<sub>2</sub> has a hexagonal atomic arrangement similar to graphene. Mo and S atoms are stacked together in a single lattice and the weak van der Waals forces exist between the

interlayers. Monolayer or bulk MoS<sub>2</sub> may have different functions due to bandgap. It has been reported that the bulk MoS<sub>2</sub> having an indirect bandgap of 1.29 eV and monolayer MoS<sub>2</sub> having a direct bandgap of 1.9 eV [9] exist in a few forms of crystal structures such as 1T-MoS<sub>2</sub> (tetragonal), 2H-MoS<sub>2</sub> (hexagonal), and 3R-MoS<sub>2</sub> (rhombohedral) [10]. As per the report by Radisavljevic et al., the pristine single crystal-based MoS<sub>2</sub> field effect transistors have shown mobility of  $200 \text{ cm}^2/\text{Vs}$  with a current on/off ratio of  $10^8$  [11]. Particularly, MoS<sub>2</sub> received special attention among the TMDCs and believed as an alternative material for graphene (which has zero bandgap) in electronics [12].

By having salient features such as nominal bandgap, good carrier mobility, and interesting geometry, MoS<sub>2</sub> rises as an important candidate material in electronics and transistor development [13]. MoS<sub>2</sub> thin films have shown tremendous potentiality in the applications such as nanogenerators, electrochemical supercapacitors, photovoltaic cells, sensors,

and detectors [14–16]. The thermal instability of nanomaterials is the unavoidable parameter for these devices, because the materials may be heated due to photon absorption, charge carrier flow, and surrounding environment which may affect the device performance. Substrate used for material deposition also plays a key role in thermal stability. Previously, it was reported that monolayer thin film on SiO<sub>2</sub> substrate is thermally stable compared to bulk MoS<sub>2</sub>. However, the preparation of large area thin film with a uniform surface is still a quite difficult process and suitable appropriate methods have to be followed. Some reports were published recently on the large area thin films which were made using physical vapor deposition (PVD), chemical vapor deposition (CVD), vapor epitaxy, pulsed-laser depositor (PLD) and sputtering methods [14, 17]. These methods involve high costs and large manpower with complicated process procedures. Hence, a simple and cost-effective method is required as an alternative. In this work, we used a hydrothermal method to produce MoS<sub>2</sub> nanoparticles and used spin-coating to make large area thin film. The hydrothermal method is a simple and cost-effective method through which good quality samples can be prepared and large area thin films can be formed by spin-coating with thickness control by standardizing the film-making procedures [18, 19].

In the recent past, only a few studies have been reported on the electrical transport properties of MoS<sub>2</sub> thin film transistors (TFT) [20, 21], and their electronic transport properties and their mechanism are not explored well and required to be investigated more. Hence in this paper, we report the simple preparation procedure of MoS<sub>2</sub> nanoparticles, thin film making, and the electrical transport characteristics of MoS<sub>2</sub> TFT in detail.

## 2. Materials and Methods

**2.1. Materials.** All the research grade materials such as molybdenum oxide (MoO<sub>3</sub>), potassium thiocyanate, HCl (35 wt%), ethanol, and NaOH were purchased from Sigma-Aldrich and used without further purification. Deionized water is used in all experiments.

**2.2. Preparation of MoS<sub>2</sub> Samples.** MoS<sub>2</sub> nanoparticles were prepared by using the hydrothermal method [18, 22] using molybdenum oxide (MoO<sub>3</sub>) and potassium thiocyanate as precursor starting materials. Initially, 0.3 g of MoO<sub>3</sub> (1.5 mmol) and 0.5 g of potassium thiocyanate (4 mmol) were dissolved in 50 mL of deionized water and the same was sonicated for 1 hr. Then, HCl solution (1 mol/L) was added in order to keep the solution pH value to 2.0, and the solution has been stirred for another 45 min. Thereafter, the solution has been transferred into a stainless-steel autoclave (Teflon-lined, 100 mL capacity) for the hydrothermal treatment at 250°C for 40 hrs. After the treatment, the system is allowed to be cooled to room temperature. Then, the centrifugation is done with 5000 rpm for 20 min resulting black colored MoS<sub>2</sub> particles which were washed several times using ethanol and DI water. Then, the sample has been put inside a vacuum oven at 70°C (10 hrs) for drying. Spin-

coating is used to prepare MoS<sub>2</sub> thin film and silver paste was used to make contact electrodes.

**2.3. Instrumentation.** The absorption spectra of MoS<sub>2</sub> nanoparticles were taken using the UV-vis spectrophotometer (model: Jasco V-670). Fourier transform infrared spectroscopy (FT-IR) was performed via FT spectrometer (model: Nicolet-6700, USA). Further, MoS<sub>2</sub> thin film was analyzed with X-ray diffractometer (model: Shimadzu, XRD 6000) with Cu-K<sub>α</sub> radiation from the range of 10–70. Raman studies were done in Raman spectrometer (model: Horiba Scientific, LabRAM). All the electrical transport analyses have been performed using the semiconductor parameter analyzer (model: Agilent, B1500A).

## 3. Results and Discussion

Surface morphology of MoS<sub>2</sub> thin film has been studied by using scanning electron microscopy (SEM), transmission electron microscopy (TEM), and atomic force microscopy (AFM) techniques.

In Figure 1(a), the SEM image of MoS<sub>2</sub> thin film is shown which clearly shows an irregular surface morphology of MoS<sub>2</sub> thin film with wrinkled-like morphology. In Figure 1(b), the TEM image of MoS<sub>2</sub> is shown which clearly depicts the sheet-like morphology with transparent nature. The 2D topography of MoS<sub>2</sub> thin film was studied by using AFM (which is shown in Figure 1(c)) which shows an average surface roughness of MoS<sub>2</sub> thin film with value of 64 nm. This roughness is due to the overlapping of many MoS<sub>2</sub> platelets so that the measured region might consist of overlapped MoS<sub>2</sub> layers.

The optical image of MoS<sub>2</sub> thin film is shown in Figure 2(a). The UV-vis spectroscopy graph as shown in Figure 2(b) reveals the absorption spectra at 208 nm. The peak observed in the near UV region is mainly caused by the excitonic characteristics of MoS<sub>2</sub> nanoparticles [23]. In order to study the chemical compositions and vibration bonds in the sample, FT-IR measurement has been done which is shown in Figure 2(c). There is a feeble absorption peak at near 470 cm<sup>-1</sup> which is ascribed to the characteristics Mo-S vibration mode and well-matched with the previous report [24].

The XRD pattern of the MoS<sub>2</sub> thin film is shown in Figure 2(d). The main characteristic diffraction peak observed at 14.5° represents the (002) plane of the hexagonal structure of MoS<sub>2</sub> and matched with the previous report [25]. Moreover, the other diffraction peaks were observed at 33°, 40°, 44°, 50°, and 61° representing the (100), (103), (005), (105), and (008) crystal planes of MoS<sub>2</sub>, respectively. This XRD data shows a good agreement with JCPDS card no. 37-1492.

### 3.1. Electrical Transport Studies

**3.1.1. Current-Voltage (I-V) Characterization of MoS<sub>2</sub> Thin Film.** The current-voltage characteristics of MoS<sub>2</sub> thin film is shown in Figure 3(a).

It shows a slight nonlinear behavior. However, a clear symmetricity has been seen in I-V curve shown in

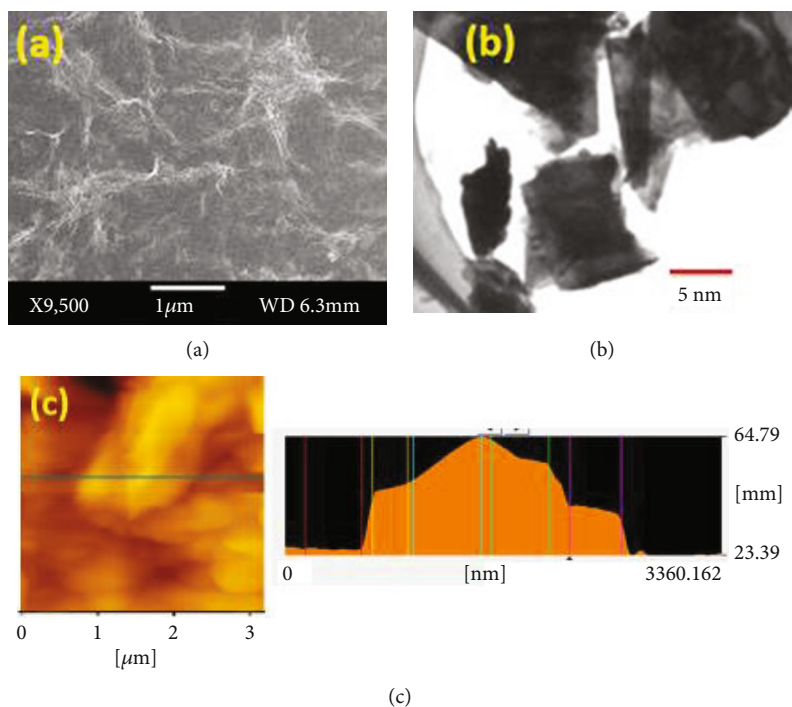


FIGURE 1: (a) SEM image of MoS<sub>2</sub> thin film. (b) TEM image of MoS<sub>2</sub> nanofilm. (c) AFM image of MoS<sub>2</sub> thin film, showing the thickness profile of 64 nm.

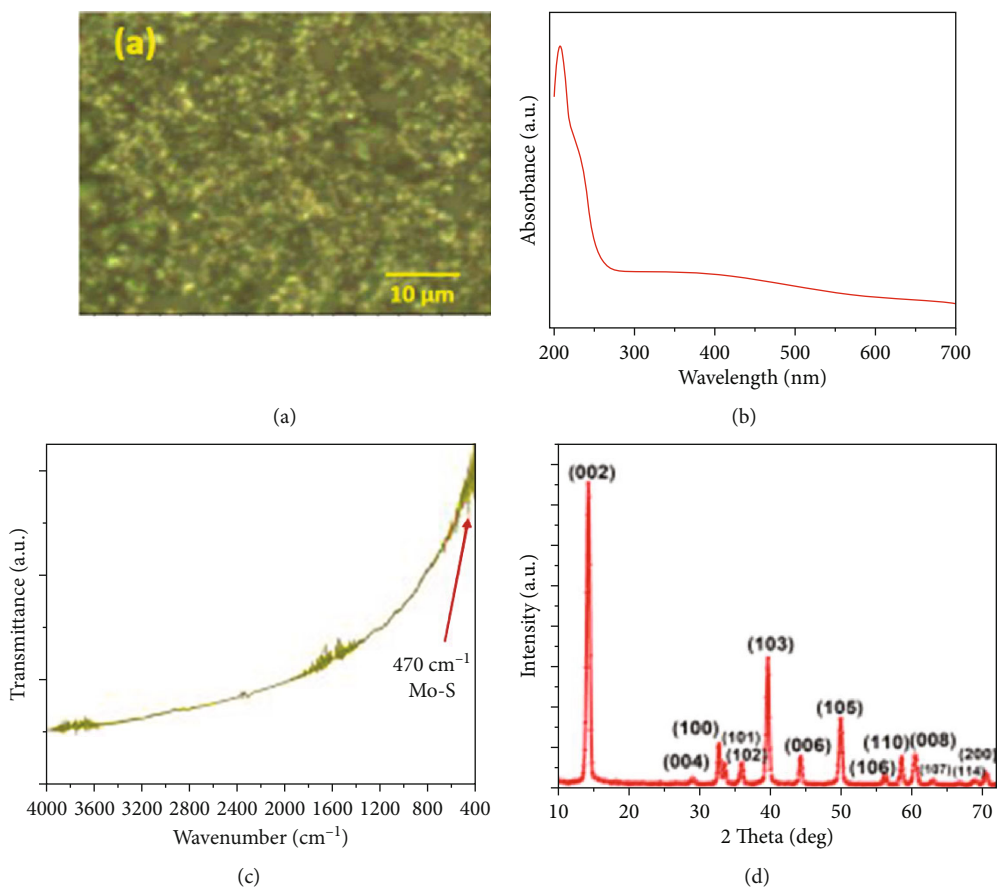


FIGURE 2: (a) Optical photograph of MoS<sub>2</sub> thin film. (b) UV-vis spectra of MoS<sub>2</sub> nanoparticles. (c) FT-IR spectra of MoS<sub>2</sub> nanoparticles. (d) XRD spectra of MoS<sub>2</sub> thin film.

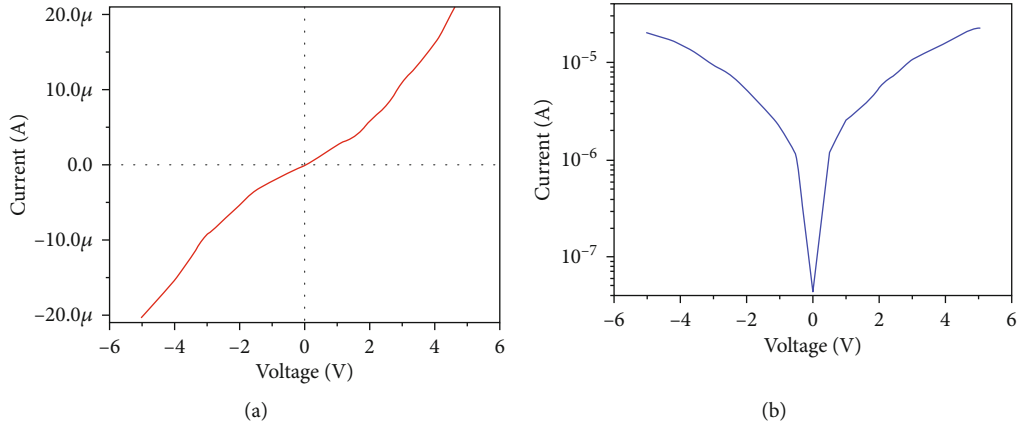


FIGURE 3: (a) Current-voltage characteristics of MoS<sub>2</sub> thin film. (b) Semilog I-V plot reveals a clear symmetry.

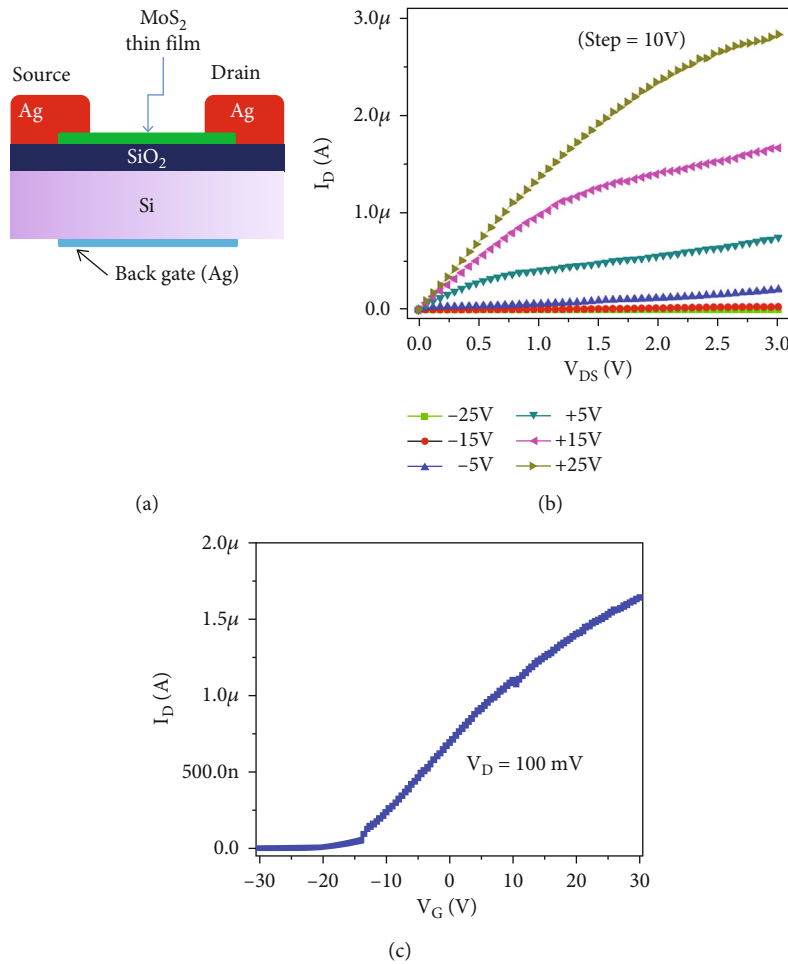


FIGURE 4: (a) The schematic of the MoS<sub>2</sub> TFT device. (b) Output characteristics ( $I_D$  versus  $V_{DS}$ ) of MoS<sub>2</sub> TFT device at different back gate voltages. An apparent linear ohmic behavior is observed. (c) Transfer characteristics ( $I_D$ - $V_G$ ) of the same device.

Figure 3(b) which further confirms the no formation of the Schottky barrier between the contacts and thin film.

**3.1.2. Characterization of MoS<sub>2</sub> Thin Film Transistor (TFT).** The schematic of the fabricated MoS<sub>2</sub> TFT device is shown in Figure 4(a).

The transistor characteristics are studied for MoS<sub>2</sub> thin film and their output characteristics ( $I_D$ - $V_{DS}$ ) for the different back-gate voltages ( $V_G$ ) varying from -25 to 25 V with a step of 10 V are shown in Figure 4(b). We observed a linear  $I_D$  versus  $V_{DS}$  curve, confirming an ohmic contact between thin film and electrodes. The transfer characteristics ( $I_D$ -

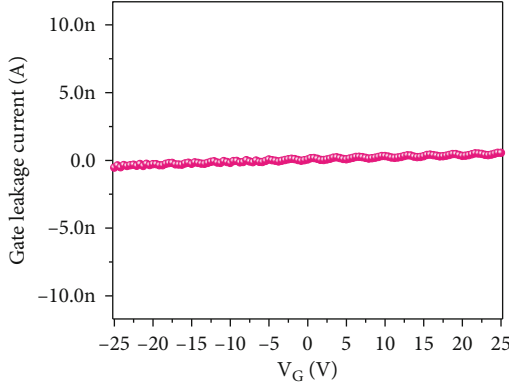


FIGURE 5: Gate leakage current versus gate bias voltage characteristics of MoS<sub>2</sub> TFT.

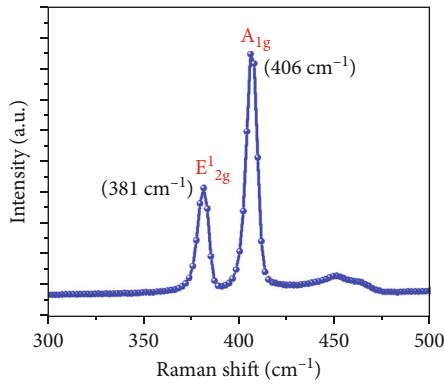


FIGURE 6: Raman spectra of MoS<sub>2</sub> thin film.

$V_G$ ) of MoS<sub>2</sub> TFT are shown in Figure 4(c), where the applied bias voltage is 100 mV.

When the gate voltage is increased, the drain current is also increased, which reveals the n-type behavior of TFT. Positive gate voltage produces more drain-current modulation than negative gate voltage ( $V_G$ ). The appearance of the charge neutrality point ( $V_{CNP}$ ) at the negative bias region ( $V_G \sim -20$  V) further concludes that the TFT device is n-doped. Figure 5 shows the relationship between gate current (IG) and gate voltage ( $V_G$ ).

This shows the negligible gate current through the SiO<sub>2</sub> oxide layer and confirms the excellent reliability of transfer characteristics presented in Figure 4(b). In addition, we extracted the mobility of our fabricated TFT device. The mobility ( $\mu$ ) of MoS<sub>2</sub> TFT was calculated using the following.

$$\mu = \frac{L \times g_m}{W \times C_{ox} \times V_d}, \quad (1)$$

where channel length ( $L$ ) is equal to 30  $\mu$ m, the channel width ( $W$ ) is equal to 25  $\mu$ m, and the capacitance between the channel and back gate per unit area is  $C_{ox}$  where  $C_{ox} = \xi_0 \xi_r / d = 3.83 \times 10^{-8}$  F/m<sup>2</sup>, where  $\xi_0$  is the permittivity of free space,  $\xi_r$  is 3.9 for SiO<sub>2</sub>, and  $d$  is gate oxide thickness

(90 nm). We determined the mobility of MoS<sub>2</sub> TFT as  $\sim 10.2$  cm<sup>2</sup>/Vs from these data. This is comparable to the mobility of multilayer MoS<sub>2</sub> transistor reported by Sharma et al. [26] where the mobility was reported as  $\mu \sim 15.3$  cm<sup>2</sup>/Vs. The reduction in mobility is due to the defects that exist in the thin film which acts as scattering centers which resist the charge conduction. The reason for the low-mobility was further supported with Raman spectra analysis which is shown in Figure 6. The Raman spectra show two active modes at 381 cm<sup>-1</sup> and 406 cm<sup>-1</sup> which represent the E<sub>12g</sub> and A<sub>1g</sub> vibration modes, respectively. Out of these two vibration modes, A<sub>1g</sub> corresponds with the thickness of the layer and A<sub>1g</sub> mode at 406 cm<sup>-1</sup> reveals that the thin film may consist of several MoS<sub>2</sub> sheets interlinked each other. As per the previous reports, the spin-coated thin films consist of several layers of MoS<sub>2</sub> and its bulk counterpart [27, 28].

In general, the surface defects and structural disorders form traps in the form of wrinkles or folds on the surface, creating a small bulk counterpart in MoS<sub>2</sub> thin film [29]. These traps are answerable for the observation of lower mobility in TFT devices. Breakage of S-Mo-S bonds during the synthesis process may lead to these kinds of traps/vacancy defects.

From the obtained results, we noticed that some sophisticated sample preparation techniques such as atomic layer deposition and chemical vapour deposition could be utilized to develop the high purity thin film for ultrafast response electronics devices.

## 4. Conclusion

The electrical transport characteristics of nanoform MoS<sub>2</sub> thin film transistor device were investigated. MoS<sub>2</sub> nanoparticles were prepared using the hydrothermal method. The as-prepared MoS<sub>2</sub> samples were characterized with UV-vis, FT-IR, and X-ray diffraction techniques. Back-gated MoS<sub>2</sub> transistor device was made with silver electrodes as a source and drain. The current-voltage characteristics show a non-linear behaviour. But the observation of symmetry in the I-V curves confirms the nonexistence of the Schottky contact between the thin film and contacts. Transistor characteristic studies further reveal that the TFT device is n-doped while registering the charge neutrality point at the negative bias region. The relationship between gate current and gate voltage with zero gate current shows the good solidarity of transfer characteristic results. The device mobility is calculated as  $\sim 10.2$  cm<sup>2</sup>/Vs, which has a well agreement with the data reported for the MoS<sub>2</sub> transistor. The observation of lower mobility in our MoS<sub>2</sub> TFT device is further plausibly explained with Raman spectra analysis.

## Data Availability

The complete data required for the representations are fully included in the research paper.

## Conflicts of Interest

The authors declare that they have no conflicts of interest.

## References

- [1] S. Kim, J. Nah, I. Jo et al., "Realization of a high mobility dual-gated graphene field-effect transistor with  $\text{Al}_2\text{O}_3$  dielectric," *Applied Physics Letters*, vol. 94, no. 6, article 62107, 2009.
- [2] K. S. Novoselov, D. Jiang, F. Schedin et al., "Two dimensional atomic crystals," *Proceedings of the National Academy of Sciences*, vol. 102, no. 30, p. 10451, 2005.
- [3] M. Chen, Y. Dai, J. Wang et al., "Smart combination of three-dimensional flower-like  $\text{MoS}_2$  nanospheres/interconnected carbon nanotubes for application in supercapacitor with enhanced electrochemical performance," *Journal of Alloys and Compounds*, vol. 696, pp. 900–906, 2017.
- [4] G. Ye, Y. Gong, J. Lin et al., "Defects engineered monolayer  $\text{MoS}_2$  for improved hydrogen evolution reaction," *Nano Letters*, vol. 16, no. 2, pp. 1097–1103, 2016.
- [5] S. V. Prabhakar Vattikuti and J. Shim, "Synthesis, characterization and photocatalytic performance of chemically exfoliated  $\text{MoS}_2$ ," *IOP Conference Series: Materials Science and Engineering*, vol. 317, no. 1, p. 12025, 2018.
- [6] M. Acerce, D. Voiry, and M. Chhowalla, "Metallic 1T phase  $\text{MoS}_2$  nanosheets as supercapacitor electrode materials," *Nature Nanotechnology*, vol. 10, no. 4, pp. 313–318, 2015.
- [7] Y. Liang, R. Feng, S. Yang, H. Ma, J. Liang, and J. Chen, "Rechargeable Mg batteries with graphene-like  $\text{MoS}_2$  cathode and ultra-small Mg nanoparticle anode," *Advanced Materials*, vol. 23, no. 5, pp. 640–643, 2011.
- [8] J. Chen, K. Nobuhiro, Y. Huatang, H. T. Takeshita, and T. Sakai, "Electrochemical hydrogen storage in  $\text{MoS}_2$  nanotubes," *Journal of the American Chemical Society*, vol. 123, no. 47, pp. 11813–11814, 2001.
- [9] A. D. Yoffe, "Electronic properties of some chain and layer compounds," *Chemical Society Reviews*, vol. 5, p. 51, 1976.
- [10] R. Suzuki, M. Sakano, Y. J. Zhang et al., "Valley-dependent spin polarization in bulk  $\text{MoS}_2$  with broken inversion symmetry," *Nature Nanotechnology*, vol. 10, no. 9, pp. 611–617, 2014.
- [11] B. Radisavljevic, A. Radenovic, J. Brivio, V. Giacometti, and A. Kis, "Single-layer  $\text{MoS}_2$  transistors," *Nature Nanotechnology*, vol. 6, no. 3, pp. 147–150, 2011.
- [12] F. Xiong, Z. Cai, L. Qu, P. Zhang, Z. Yuan, and O. K. Asare, "Three-dimensional crumpled reduced graphene oxide/ $\text{MoS}_2$  nanoflowers: a stable anode for lithium-ion batteries," *ACS Applied Materials & Interfaces*, vol. 7, no. 23, pp. 12625–12630, 2015.
- [13] J. Yuan and J. Lou, "Memristor goes two-dimensional," *Nature Nanotechnology*, vol. 10, no. 5, pp. 389–390, 2015.
- [14] P. Qin, G. Fang, W. Ke et al., "In situ growth of double-layer  $\text{MoO}_3/\text{MoS}_2$  film from  $\text{MoS}_2$  for hole-transport layers in organic solar cell," *Journal of Materials Chemistry A*, vol. 2, no. 8, pp. 2742–2756, 2014.
- [15] H. Zhu, Y. Wang, J. Xiao et al., "Observation of piezoelectricity in free-standing monolayer  $\text{MoS}_2$ ," *Nature Nanotechnology*, vol. 10, no. 2, pp. 151–155, 2015.
- [16] O. Lopez-Sanchez, D. Lembke, M. Kayci, A. Radenovic, and A. Kis, "Ultrasensitive photodetectors based on monolayer  $\text{MoS}_2$ ," *Nature Nanotechnology*, vol. 8, no. 7, pp. 497–501, 2013.
- [17] L. Ma, D. N. Nath, E. W. Lee II et al., "Epitaxial growth of large area single-crystalline few-layer  $\text{MoS}_2$  with high space charge mobility of  $192\text{ cm}^2\text{ V}^{-1}\text{ s}^{-1}$ ," *Applied Physics Letters*, vol. 105, no. 7, article 72105, 2014.
- [18] N. Chaudhary, M. Khanuja, and S. S. I. Abid, "Hydrothermal synthesis of  $\text{MoS}_2$  nanosheets for multiple wavelength optical sensing applications," *Sensors and Actuators A: Physical*, vol. 277, pp. 190–198, 2018.
- [19] L. Luo, M. Shi, S. Zhao et al., "Hydrothermal synthesis of  $\text{MoS}_2$  with controllable morphologies and its adsorption properties for bisphenol A," *Journal of Saudi Chemical Society*, vol. 23, no. 6, pp. 762–773, 2019.
- [20] S. Kim, A. Konar, and W. S. Hwang, "High-mobility and low-power thin-film transistors based on multilayer  $\text{MoS}_2$  crystals," *Nature Communications*, vol. 3, p. 1011, 2012.
- [21] J. Pu, Y. Yomogida, K. Liu, L.-J. Li, Y. Iwasa, and T. Takenobu, "Highly flexible  $\text{MoS}_2$  thin-film transistors with ion gel dielectrics," *Nano Letters*, vol. 12, no. 8, pp. 4013–4017, 2012.
- [22] L. Luo, J. Li, J. Dai et al., "Bisphenol A removal on  $\text{TiO}_2$ - $\text{MoS}_2$ -reduced graphene oxide composite by adsorption and photocatalysis," *Process Safety and Environmental Protection*, vol. 112, pp. 274–279, 2017.
- [23] V. Chikan and D. Kelley, "Size-dependent spectroscopy of  $\text{MoS}_2$  nanoclusters," *Journal of Physical Chemistry B*, vol. 106, no. 15, pp. 3794–3804, 2002.
- [24] D. Gao, M. Si, J. Li et al., "Ferromagnetism in freestanding  $\text{MoS}_2$  nanosheets," *Nanoscale Research Letters*, vol. 8, p. 129, 2013.
- [25] K. Chan and W. Chen, "In situ synthesis of  $\text{MoS}_2$ /graphene nanosheet composites with extraordinarily high electrochemical performance for lithium ion batteries," *Chemical Communications*, vol. 47, pp. 4252–4254, 2011.
- [26] D. Sharma, A. Motayed, P. B. Shah et al., "Transfer characteristics and low-frequency noise in single- and multi-layer  $\text{MoS}_2$  field-effect transistors," *Applied Physics Letters*, vol. 107, p. 162102, 2015.
- [27] C. Lee, H. Yan, L. E. Brus, T. F. Heinz, J. Hone, and S. Ryu, "Anomalous lattice vibrations of single- and few-layer  $\text{MoS}_2$ ," *ACS Nano*, vol. 4, no. 5, pp. 2695–2700, 2010.
- [28] S. Baidyaroy and P. Mark, "Analytical and experimental investigation of the effects of oxygen chemisorption on the electrical conductivity of  $\text{CdS}$ ," *Surface Science*, vol. 30, no. 1, pp. 53–68, 1972.
- [29] H. C. Schniepp, J. L. Li, M. J. McAllister et al., "Functionalized single graphene sheets derived from splitting graphite oxide," *Journal of Physical Chemistry B*, vol. 110, no. 17, pp. 8535–8539, 2006.